

# High Ram Acceleration Using Open-Base Projectile

Yuichiro Hamate,\* Akihiro Sasoh,<sup>†</sup> and Kazuyoshi Takayama<sup>‡</sup>  
Tohoku University, Sendai 980-8577, Japan

High-acceleration operation has been realized in a 25-mm-bore ram accelerator by employing an open-base projectile. The projectile comprises a centerbody and four fins like a conventional ram accelerator projectile, but is manufactured as a single piece. The base of the centerbody is perforated so that pressures inside and outside are almost balanced, thereby reducing the required thickness of the centerbody wall and the total mass. Reliable ram acceleration could be started only when the entrance velocity was increased by 0.1 km/s from that set for the conventional projectile. Although the propellant fill pressure was as modest as 3.5 MPa, an average acceleration of  $4.4 \times 10^4 g$  and a velocity increment of 1.0 km/s have been achieved through a 4.1-m-long, three-stage ram acceleration section.

## Nomenclature

$A$	=	tube cross-sectional area
$a$	=	speed of sound
$F$	=	thrust
$h$	=	specific static enthalpy
$M$	=	projectile Mach number
$M_i$	=	entrance projectile Mach number in $i$ -th stage
$m_o$	=	mass of obturator
$m_p$	=	mass of projectile
$P$	=	pressure
$Q$	=	dimensionless heat release
$q$	=	specific heat release
$t$	=	time
$U$	=	projectile velocity
$U_{CJ}$	=	Chapman–Jouguet detonation velocity
$X$	=	methane mole number with respect to $2O_2$
$x$	=	travel distance from the entrance of ram acceleration section
$Y$	=	diluent mole number with respect to $2O_2$
$\gamma$	=	specific heat ratio
$\eta$	=	ballistic efficiency, Eq. (1)
$\rho$	=	density
$\tau_m$	=	characteristic time for obturator separation

## Introduction

A RAM accelerator is an important ballistic range device that is capable of high ballistic efficiency because a large thrust can be applied over the entire acceleration period. Its operation was first experimentally demonstrated at the University of Washington.<sup>1</sup> Investigations on performance characteristics emphasizing a hypervelocity, heavy-mass launcher followed.<sup>2–5</sup> In particular, operation with a bore of up to 120 mm was realized.<sup>2,3</sup> Fundamental investigations on the thrust production mechanisms using various tube/projectile configurations and dimensions have also been conducted.<sup>6–11</sup> Although the facility dimension is largely budget dependent, the projectile acceleration level is not explicitly subject to this constraint. The square-cubic law states that the force scales with the square

of a dimension and the mass with its cube; if this law holds, high acceleration and velocity can be realized in even a small facility. There are three methods to increase the acceleration: 1) multistage operation, 2) increasing the propellant fill pressure, and 3) decreasing the projectile mass.

The effectiveness of the first method has already been experimentally validated by many researchers.<sup>1,5,11–13</sup> This scheme is currently in routine use. In particular, at the University of Washington, a muzzle velocity of 2.7 km/s through a 38-mm-bore, 16-m-long, four-stage ram acceleration section has been achieved.<sup>14</sup>

Using the second method, Bundy et al.<sup>15,16</sup> conducted experiments with elevated fill pressures of up to 20 MPa. However, the projectile acceleration does not increase linearly with the fill pressure due to the following three problems. First, with the increased fill pressures, ram acceleration tends to be delayed. Here, ram acceleration implies a process that generates a positive thrust to the projectile with the ignition of the compressed mixture around the projectile aftbody. Second, the measured thrust is smaller than that predicted for thermally choked operation.<sup>17,18</sup> Here, thermally choked operation is defined as the ram accelerator operation in which the flow becomes choked behind the projectile where the heat release of the combustion terminates. Third, because the pressure around the projectile also increases, the projectile wall needs to be thicker; the thrust to projectile mass ratio cannot simply be increased.

Thus far, the third method, that is, making a projectile lighter, has not been examined intensively. This method can be effective even if the propellant fill pressure is limited to a moderate value. The present study emphasizes this aspect in ram accelerator operation by experimentally examining operation characteristics of newly developed, ultralight projectiles named open-base projectiles.

## Open-Base Projectile

Most projectiles used in previous ram accelerator studies have had a centerbody, which is supported either by fins<sup>1,5,8,10,12,13</sup> or rails.<sup>7</sup> Although other shapes have been examined, including an internal-flow hollow projectile,<sup>19</sup> a planar (quasi-two-dimensional) projectile in a circular tube,<sup>20</sup> and a two-dimensional projectile in a rectangular ram acceleration section,<sup>9,21</sup> to date the centerbody shape has exhibited the best performance and reliability. In ram accelerator operation at the ISL, French–German Research Institute of Saint Louse,<sup>7</sup> the projectile was preaccelerated using a powder gun up to a superdetonative velocity of the order of 1.8 km/s. The average acceleration in the 2.8-m-long prelauncher was about  $6 \times 10^4 g$ ; the peak acceleration was estimated to be two to three times higher. For the projectile to keep its integrity during the prelaunch at this high-acceleration level, it was manufactured as a single piece. On the other hand, for thermally choked operation, the required entrance velocity is about 1.2 km/s, and the projectile experiences an acceleration level usually up to  $4 \times 10^4 g$  throughout the process. At this acceptable acceleration level, the centerbody can be hollowed.

Received 22 May 2002; revision received 19 October 2002; accepted for publication 21 October 2002. Copyright © 2002 by the authors. Published by the American Institute of Aeronautics and Astronautics, Inc., with permission. Copies of this paper may be made for personal or internal use, on condition that the copier pay the \$10.00 per-copy fee to the Copyright Clearance Center, Inc., 222 Rosewood Drive, Danvers, MA 01923; include the code 0748-4658/03 \$10.00 in correspondence with the CCC.

\*Postdoctoral Fellow, Institute of Fluid Science, 2-1-1 Katahira, Aoba; sasoh@ifs.tohoku.ac.jp. Associate Fellow.

<sup>‡</sup>Professor, Institute of Fluid Science, 2-1-1 Katahira, Aoba; takayama@ifs.tohoku.ac.jp. Senior Member AIAA.

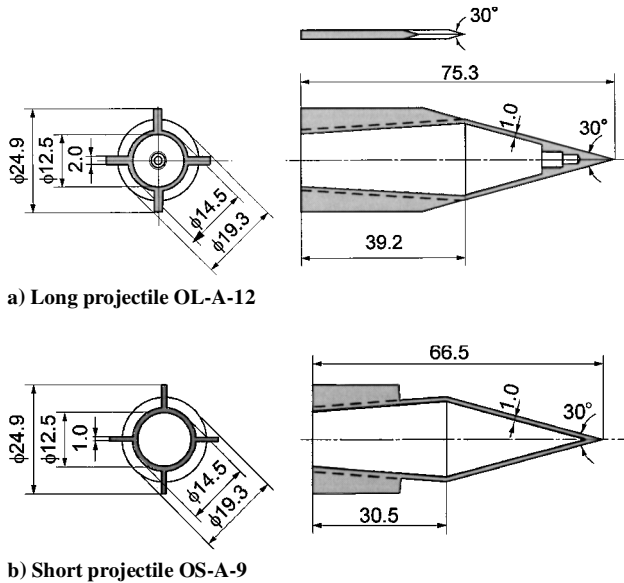


Fig. 1 Open-base projectiles.

Usually the hollow is machined by dividing a projectile into two pieces, a nose and an aftbody. After machining a hollow in each piece, the two pieces are threaded together. In this way, the mass of the projectile is decreased.<sup>1</sup> However, while the pressure outside of the centerbody becomes 20 times as high as the fill pressure or higher, the inside pressure remains unchanged during the operation. Therefore, this type of projectile experiences a large compressive mechanical load from the outside, against which this vessel is weak in nature. Moreover, in this shape the thread can cause a decrease in the effective strength per unit cross-sectional area or inefficient projectile mass reduction.

Hamate et al.<sup>22</sup> proposed a new projectile design, an open-base projectile to increase the acceleration with a limited operation pressure. When the centerbody base is perforated, pressures inside and outside the projectile are almost balanced. The wall thickness of the centerbody can be significantly reduced. A thread such as that used in the conventional two-piece projectile is not necessary. As described in their first publication (see Fig. 1b, Ref. 22), the ram acceleration using this open-base projectile was realized not in a steady-state manner but only during a transient period. Almost at the same time, Bundy et al.<sup>15</sup> designed for the same purpose a single-piece centerbody projectile with a clearance hole having a constant diameter in the base. They examined ram accelerator operation with a propellant fill pressure as high as 20 MPa (Ref. 15). Only when the projectile mass was reduced because of this hole, an entrance velocity high enough to start ram acceleration was obtained.

Figures 1a and 1b show the long (Fig. 1a) and short (Fig. 1b) open-base projectiles used in this study where the length is given in millimeters. They are made as a single piece, either of magnesium alloy, AZ31F, or of aluminum alloy, A7075-T6. In Figs. 1a and 1b, only projectiles made of the aluminum alloy are shown. The minimum centerbody thickness is 1 mm. Four fins support the centerbody. The projectile shown in Fig. 1a is open-base, long aftbody (OL), aluminum alloy, 12-g weight class (OL-A-12). The projectile of Fig. 1b is an open-base, shorter aftbody and fins, (OS), aluminum alloy, 9-g weight class (OS-A-9). The short projectile is also made of the magnesium alloy (not shown in Fig. 1). In this case, the thicknesses both of the centerbody and of the fins are 2 mm. The projectile is magnesium alloy, 10-g weight class (OS-M-10). The average clearance between the fins and the ram acceleration tube wall ranges 25–50  $\mu\text{m}$ . The OL projectiles exhibited better in-tube stability than the OS projectile.

### Experimental Facility

The experiments were conducted using the ram accelerator at the Shock Wave Research Center, Institute of Fluid Science, Tohoku

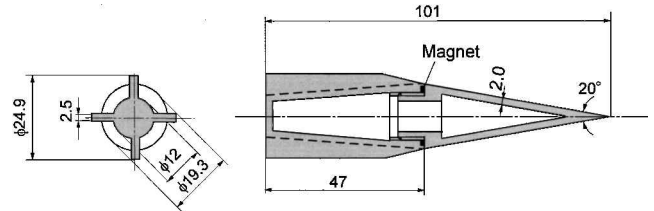


Fig. 2 Conventional projectile C-M-18.

University (RAMAC25). The bore diameter was 25 mm. A powder gun was used as the prelauncher, where the projectile was accelerated to a maximum velocity of 1.3 km/s. In the prelauncher, the projectile was backed by a perforated obturator, which in turn was backed by a backplate that plugged the perforation. The obturator assists the initiation of the ram acceleration by moderately compressing the mixture on the entry.<sup>8</sup> There are two alternative configurations of the ram acceleration section. Ram acceleration section A (the same as that presented in Ref. 8) consists of three 2-m-long tubes, along with a combination of a pressure transducer and a pick-up coil (the instrumentation unit), which are placed at a separation distance of about 0.4 m. Ram acceleration section B is designed for operation at higher acceleration. It consists of a 0.6-m-long entrance tube followed by five 1.2-m-long tubes. The instrumentation units are placed with a separation distance of 0.3 m. When the projectile passage is sensed using the pick-up coils, the projectile velocity is determined by the time-of-flight method. The facility is described in further detail in the previous papers.<sup>8,23</sup>

In the present paper, some operational characteristics of the open-base projectiles are compared with those of a conventional projectile (C-M-18) shown in Fig. 2, with length given in millimeters. It comprises two pieces (a nose and an aftbody), which are threaded together. The projectile is made of the magnesium alloy and weighs 18.5 g.

The ram accelerator performance itself was sensitive to various environmental factors, including room temperature, projectile loading conditions, and small variations in the projectile entrance velocity. Based on previous ram accelerator experiments, the error margin of the mixture composition is taken to be of the order of 5%. To obtain higher accuracy of mixture composition, the molar ratios of the respective species were re-examined using a gas chromatograph (GC-14B, C-R5a, Shimadzu). The accuracy in the molar ratios was kept to better than 2%, which is small enough to satisfy the mentioned error margin.

Ram accelerator operation experiments cannot be conducted very frequently. At our normal staffing level, one shot per day was close to the practical limit. For an important operation condition, the reliability of the experimental results was validated by repeating the experiments under the same conditions. However, with so many independent parameters to examine, the same conditions could not always be replicated. Even in such a case, after examining several operation conditions that were slightly different from each other, the consistency of the measured results could be examined.

### Reliable Starting Condition

There exists a difference in ram acceleration starting characteristics between the conventional projectile and the open-base projectile. Entrance velocities that are sufficient to initiate ram acceleration with a conventional projectile may be inadequate for the open-base projectile; the ram acceleration may be delayed or may fail entirely. Figure 3 shows projectile velocity histories, with the same mixture and an equal entrance velocity, using either a conventional or an open-base projectile. Here,  $U$  designates the projectile velocity and  $x$  the travel distance from the entrance of the ram accelerator section. The projectile was injected into the reliable starting mixture for the conventional projectile,  $2.8\text{CH}_4 + 2\text{O}_2 + 5.7\text{N}_2$  (Refs. 8, 12, and 24). The initial fill pressure was 3.5 MPa. The experiments were conducted in the ram acceleration section A. When the conventional projectile C-M-18 was used, ram acceleration began immediately after the projectile entered the ram acceleration section; the

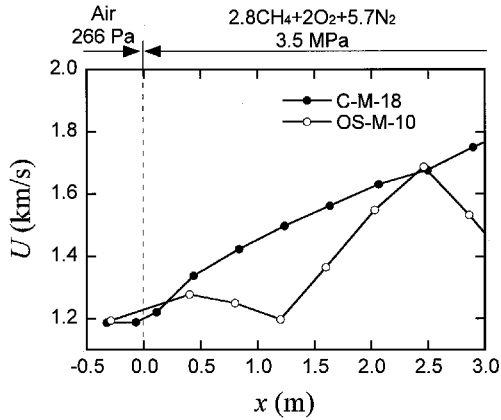


Fig. 3 Projectile velocity variations with different projectiles.

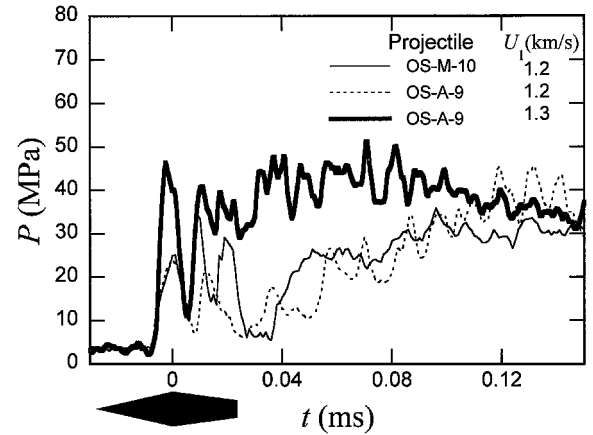


Fig. 5  $P$  histories measured at  $x = 0.6$  m for open-base projectiles, using  $2.8\text{CH}_4 + 2\text{O}_2 + 5.7\text{N}_2$ ; projectile shape corresponds to passage at location of pressure measurement with  $U_1 = 1.3$  km/s.

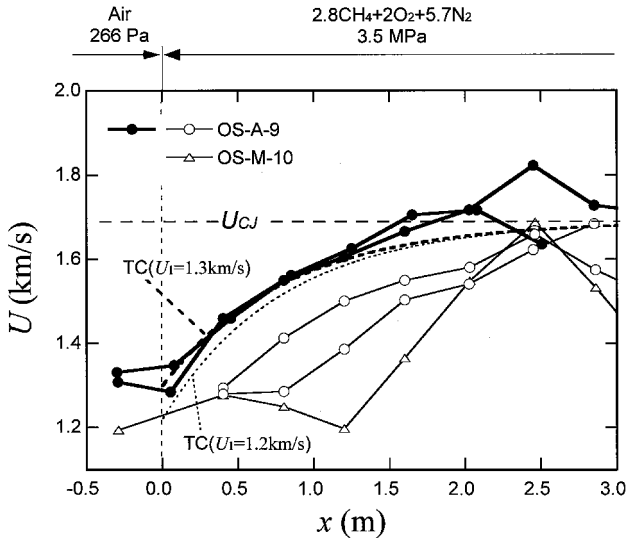


Fig. 4 Velocity variations with different entrance velocities, using open-base projectiles: TC stands for thermally choked profile.  $U_{CJ}$  is calculated for equilibrium flow.

projectile velocity continuously increased. In the case of the open-base projectile OS-M-10, immediately after entering the ram acceleration section the projectile accelerated slightly and then decelerated. Even without igniting the mixture, when entering the ram acceleration section the obturator drove a shock wave, thereby exerting a thrust onto the projectile. However, without the ignition this positive thrust was only applied near the entrance. Even at 0.6 m from the entrance, the obturator-driven shock wave does not influence the pressure field around the projectile.<sup>8</sup> In other words, the shock wave falls off from the aftbody of the projectile (wave fall-off<sup>24–26</sup>). The mixture is ignited far behind the projectile. After the projectile travels more than 1 m in the ram acceleration section, the combustion-driven shock wave catches up with the projectile and finally overtakes it (wave unstart<sup>24–26</sup>). Before the wave unstart, a positive thrust is produced only in the short zone of  $1.2 < x < 2.5$  m.

In Fig. 4, projectile velocity histories of open-base projectiles at different entrance velocities are plotted. The delay for ram acceleration was reproduced with an entrance velocity level of 1.2 km/s. However, when the velocity was increased to 1.3 km/s, ram acceleration started right after the entry; the velocity variation became consistent with the thermally choked performance.<sup>17,18</sup> These results are consistent with the pressure histories shown in Fig. 5, where  $U_1$  is the entrance velocity to the single-stage ram acceleration-section (at  $\alpha = 0$ ) and  $t = 0$  corresponds to the passage of the projectile throat, the location of the longest diameter in the centerbody. In Fig. 5, the projectile location given for  $U_1 = 1.3$  km/s is shown with the black centerbody shape. In the present experiment, it was not possible to fabricate a magnet that

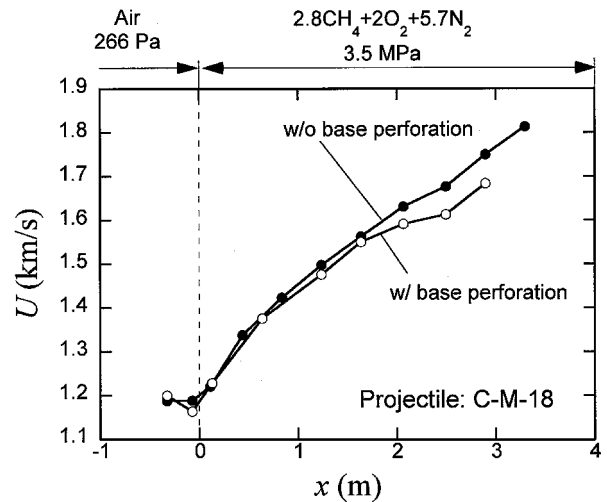


Fig. 6 Velocity variations with and without base perforation for projectile C-M-18.

could be placed onboard the projectile to detect its passage. The location of the first reflection of a conical shock emanating from the apex of the projectile nose was assumed to be equal to that calculated by solving the differential equation derived by Taylor and Maccoll.<sup>27</sup> In the case of the high-velocity entry, high pressure was maintained around the projectile aftbody, corresponding to thermally choked operation.<sup>7</sup> However, for the low-velocity entry, the pressure was substantially decreased. A dip in the pressure appeared directly behind the projectile base. The high-pressure region was separated from and somewhat behind the projectile. This is a typical pressure variation of the wave fall-off operation.

A question arises as to the cause of the delay in ram acceleration with the open-base projectiles: Is this the effect of the base perforation, mass reduction, or something else? The effect of the perforation cannot be directly examined with the present open-base configuration because a projectile of the same shape with its base plugged cannot be manufactured. Figure 6 shows projectile velocity histories measured with the conventional projectiles C-M-18 either with or without perforating the projectile base with an 8-mm-diam hole on the center axis. In this case, significant starting delay due to the base perforation was not observed. With these limited data, it is supposed that the base perforation itself does not significantly affect the delay in the start of ram acceleration.

Here, the mechanical characteristic time of the obturator separation is estimated as the period during which the obturator becomes separated from the projectile by one bore diameter. This period is regarded as a characteristic duration time for holding a high temperature/pressure slug behind the projectile. This characteristic

time is inversely proportional to the sum of the obturator deceleration and the projectile acceleration. In Ref. 8, the characteristic time was estimated neglecting the projectile acceleration and was designated as  $\tau_m$ . From the analysis of obturator separation dynamics presented in Ref. 8, the deceleration of an obturator (mass of 4.1 g and ratio of perforated to total cross-sectional area 0.46) at the entry was calculated to be  $4.5 \times 10^5$  g for an entrance velocity of 1.3 km/s and  $3.9 \times 10^5$  g for 1.2 km/s. The measured projectile acceleration was an order of magnitude smaller;  $\tau_m$  decreased only by about 5% due to the projectile acceleration. The difference in  $\tau_m$  between for the two entrance velocities was even smaller. It follows from these results that it is not likely that this delay in ram acceleration is mainly caused by the decrease in  $\tau_m$ .

A similar delay in ram acceleration was also observed by Bundy et al.<sup>15</sup> In their experiments, the fill pressure was increased beyond 10 MPa. The achieved acceleration level almost equaled that of the present study. The reason for this delay remains an open question, warranting further investigations.

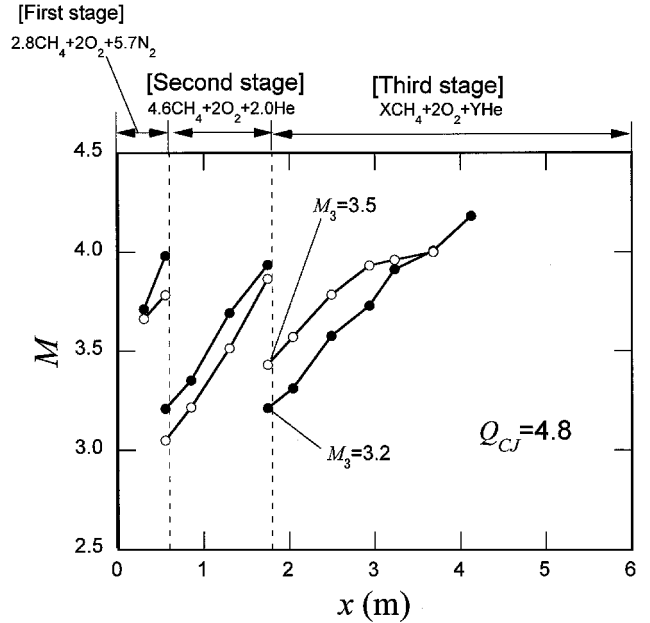
### Multistage Operation

Three-stage operation using an open-base projectile was realized in the ram acceleration section B. The open-base projectile OL-A-12 was used because, with its longer and thicker fins, it has better in-tube stability than OS-A-9. In all of the stages, the mixture fill pressure was 3.5 MPa. The first stage (0.6 m in length) was filled with the standard starting mixture,  $2.8\text{CH}_4 + 2\text{O}_2 + 5.7\text{N}_2$ . In determining the second and the third-stage mixture conditions, the Higgins et al.<sup>24</sup> and the Schultz et al.<sup>26</sup>  $Q$ - $M$  scheme was employed. In this scheme, a ram acceleration operational regime is identified in the  $Q$ - $M$  plane, where  $Q$  is the dimensionless heat release in equilibrium, or the second Damköhler number, and  $M$  is the projectile Mach number. Values of  $Q$  and  $M$  in the operational regime were obtained from an experimental database. The parameters to be determined are the species of diluent and the relative mole numbers of the fuel (methane),  $X$ , and the diluent,  $Y$ , to  $2\text{O}_2$ . Once the species of the diluent is given,  $Q$  and  $M$  at the entrance are calculated from  $X$  and  $Y$  for a given entrance velocity. Because operational  $Q$ - $M$  conditions are not uniquely determined, the actual mixture function must be determined by trial-and-error experiments. In this way,  $4.6\text{CH}_4 + 2\text{O}_2 + 2\text{He}$  was selected as the second-stage mixture.

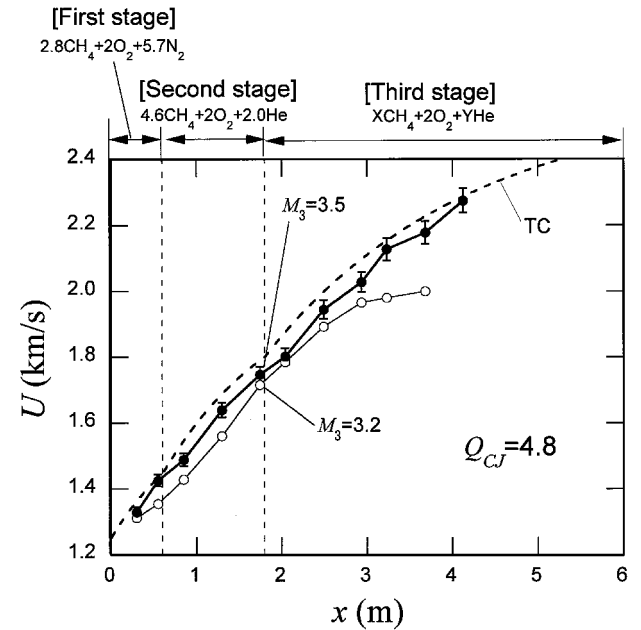
Figure 7 shows projectile velocity variations measured using five different fuel mixtures in the third stage (4.8 m long). The characteristics of the mixtures are listed in Table 1. The entrance Mach number in the third stage,  $M_3$ , was about 3.5. For  $Q = 3.4$ , wave fall-off occurs right after entering the third stage. With  $Q = 4.2$ , ram

**Table 1** Third-stage mixture characteristics in the experiments shown in Fig. 7

$X$	$Y$	$a$ , km/s	$\gamma$	$U_{CJ}$ , km/s	$Q_{CJ}$	$M_3$
3.2	4.2	0.50	1.43	2.4	5.0	3.5
3.3	4.3	0.50	1.43	2.4	4.8	3.5
3.5	4.4	0.50	1.43	2.3	4.6	3.5
4.4	4.6	0.50	1.42	2.2	4.2	3.4
8.0	6.0	0.50	1.40	1.8	3.4	3.4



a) Projectile Mach number variations



b) Projectile velocity variations

**Fig. 8** Mach number and velocity variations in three-stage, operation for two entrance Mach numbers,  $M_3$ , with projectile OL-A-12.

acceleration lasted for the longest distance. However, the average acceleration was lower than that with  $Q = 4.6$ . With  $Q$  larger than this value, wave unstart<sup>24,26</sup> occurs before reaching the achievable velocity.

However, when  $M_3$  was decreased from 3.5 to 3.2, as is seen in Fig. 8a, the effective acceleration length increased, and a higher velocity was achieved (see Fig. 8b). With this decreased value of  $M_3$ , not only the maximum velocity but also the maximum Mach

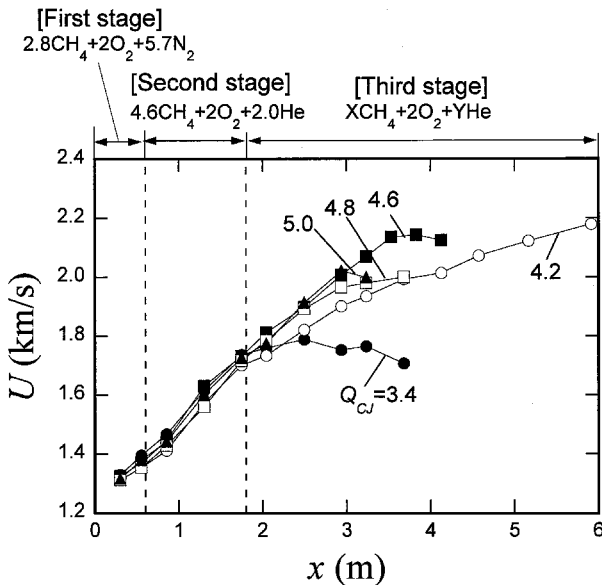


**Fig. 7** Velocity profiles for three-stage operation, using projectile OL-A-12 and a fill pressure of 3.5 MPa.

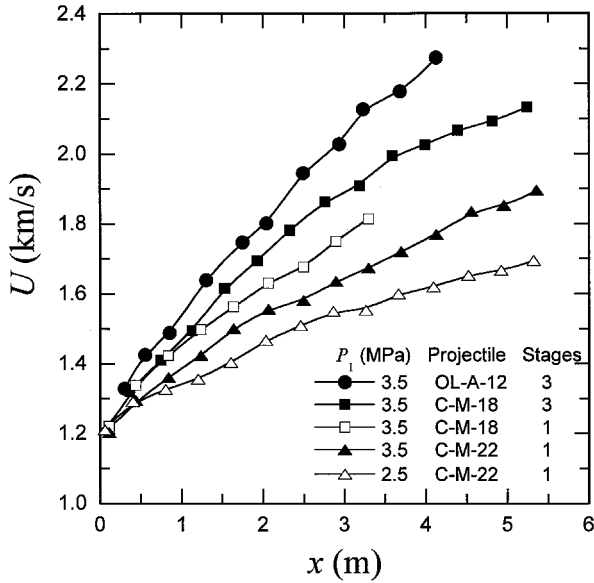


Fig. 9  $U$  vs  $x$  displaying the significance of projectile mass reduction and mixture pressure increase.

number (Fig. 8a) became higher. Between these cases, the lower  $M_3$  operation was superior to that in the earlier mentioned acceleration performance. However, note that usually starting reliability was improved with increasing the entrance Mach number. The value of 3.2 for the entrance Mach number was close to this critical condition. Hence, case-by-case propellant tuning is still necessary for other conditions.

Operation of the system at  $M_3 = 3.2$  in Fig. 8 yielded the highest performance: Through the 4.1-m-long, three-stage ram acceleration section, a velocity increment from 1.3 to 2.3 km/s and an average acceleration of  $4.4 \times 10^4$  g was achieved. The broken line in Fig. 8b represents the velocity profile that was calculated assuming thermally choked operation<sup>17</sup> throughout the section. Note that the thermally choked performance is calculated irrespective of the shape of a projectile. As is seen in Fig. 8, even with the open-base projectile, the measured velocity profile agrees well with this thermally choked performance.

Figure 9 summarizes the significance of the performance improvement due to the reduction of the projectile mass. For reference, the performance data of conventional projectiles that have been measured in the same facility are also plotted. With the conventional projectiles, the projectile acceleration has been improved by increasing the fill pressure, decreasing the projectile mass, and employing multistage operation. Further reducing the projectile mass by employing the open-base projectile resulted in an increment in the average projectile acceleration by 50% from that best obtained using the C-M-18 projectile in the three-stage operation (average acceleration,  $2.9 \times 10^4$  g). This increment in the average acceleration is consistent with the decrease in the projectile mass from 18 to 12 g.

In Fig. 10 (black symbols), single-, two- and three-stage operations using a projectile of OL-A-12 are plotted in another way. For the OL-A-12 projectile, the length and mixture for the first stage was 0.6 m and  $2.8\text{CH}_4 + 2\text{O}_2 + 5.7\text{N}_2$ ; for the second stage, 1.2 m and  $4.6\text{CH}_4 + 2\text{O}_2 + 2.0\text{He}$ ; and for the third stage, 4.8 m and  $2.9\text{CH}_4 + 2\text{O}_2 + 6.3\text{He}$ . Here, a local ballistic efficiency  $\eta$  is defined by<sup>21</sup>

$$\eta = \frac{\frac{1}{2}m_p[U(x)^2 - U(0)^2]}{\int_0^x \rho(h+q)A dx + \frac{1}{2}m_o U(0)^2} \quad (1)$$

In this expression,  $h$ ,  $q$ , and  $\rho$  designate the static enthalpy, specific heat release, and density of the mixture under the fill condition, respectively.  $U(x)$  is the projectile velocity at a distance  $x$ , which is measured from the entrance of the ram acceleration section. The

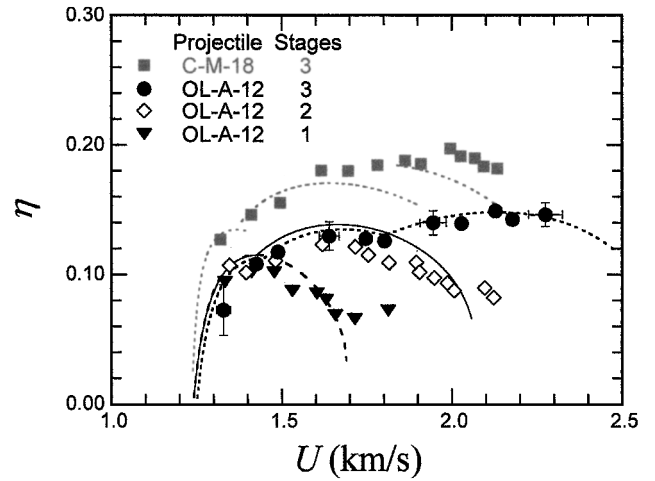


Fig. 10 Variations of ballistic efficiency in one- to three-stage operations using a fill pressure of 3.5 MPa: — and --- plot thermally-choked profiles.

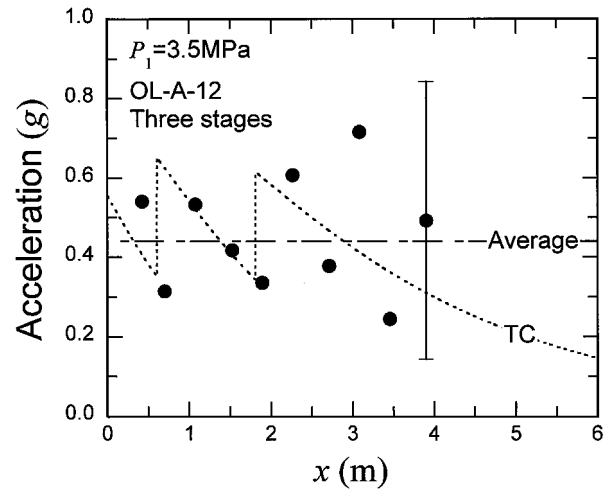


Fig. 11 Acceleration variation in the same three-stage operation using the open-base projectile as shown in Fig. 10. TC stands for thermally choked profile.

first term in the denominator is the integrated energy available from the mixture; the second term is the kinetic energy of the obturator at its entry. The latter is particularly important in estimating the energy balance immediately after the entry. As  $x$  increases, its contribution becomes less and less important. In each stage,  $\eta$  maintains an almost constant value and then starts to decrease. However, through the successful stage transitions, it can be kept at a high level as the final velocity is achieved. As seen in Fig. 10,  $\eta$  variation exhibits a small scatter in comparison with its acceleration profile (Fig. 11). This is mainly because the calculation of  $\eta$  does not involve differentiation using a limited number of  $x-t$  data, unlike the calculation for the acceleration.

Also in Fig. 10 is plotted the variation of another three-stage operation using the heavier, conventional projectile C-M-18. For the C-M-18 projectile lengths and mixtures were as follows: first stage, 0.6 m,  $2.8\text{CH}_4 + 2\text{O}_2 + 5.7\text{N}_2$ ; second stage, 2.0 m,  $4.2\text{CH}_4 + 2\text{O}_2 + 3.4\text{He}$ ; and third stage, 4.0 m,  $4.0\text{CH}_4 + 2\text{O}_2 + 9.3\text{He}$ . In this case,  $\eta$  became higher. When the wall friction is neglected, the numerator of Eq. (1) equals

$$\int_0^x F(U) dx$$

Because in the thermally choked operation  $F$  is a decreasing function of  $U$  (Ref. 17), the lower the acceleration, the higher  $\eta$  becomes. This characteristic becomes important for practical applications of the ram accelerator as a heavy-mass launcher. On the other hand,

in principle the high-acceleration operation sacrifices ballistic efficiency. However, the high-acceleration capability that has been demonstrated in the present study would become useful in a facility of limited dimensions. In general, depending on the purpose of ram accelerator operation, the operation condition should be determined from the tradeoff between these aspects.

### Conclusions

In the present study, it has been demonstrated that high ram acceleration can be realized by significantly reducing the projectile mass using open-base projectiles. When the open-base projectile was used, the average acceleration was increased by 50% of the best value obtained using the conventional projectile. Through the 4.1-m-long, three-stage ram acceleration section, an average acceleration of  $4.4 \times 10^4$  g and a maximum velocity of 2.3 km/s was achieved. Even at this high-acceleration level, an overall ballistic efficiency of 0.15 was attained. With this light projectile, the projectile entrance velocity needs to be increased to at least 1.3 km/s to avoid the delay for the ram acceleration. Through the presented results, the functional flexibility of the ram accelerator has been demonstrated to be high. To explore the possibility of increasing the muzzle velocity, increasing the length of the ram acceleration tube is not the only solution. Such high-acceleration operation using the ultralight projectiles is useful, in particular, in a facility of modest dimensions.

### Acknowledgements

The authors would like to thank O. Onodera, H. Ojima, and T. Ogawa of the Shock Wave Research Center, for their technical support. We are also grateful for the efforts at manufacturing the projectiles and other related items made by M. Kato, K. Asano, and K. Takahashi of the machine shop of the Institute of Fluid Science.

### References

- <sup>1</sup>Hertzberg, A., Bruckner, A. P., and Bogdanoff, D. W., "Ram Accelerator: A New Chemical Method for Accelerating Projectiles to Ultrahigh Velocities," *AIAA Journal*, Vol. 26, No. 2, 1988, pp. 195–203.
- <sup>2</sup>Kruczynski, D. L., and Nusca, M. J., "Experimental and Computational Investigation of Scaling Phenomena in a Large Caliber Ram Accelerator," AIAA Paper 92-3245, 1992.
- <sup>3</sup>Kruczynski, D. L., "High Performance Ram Accelerator Research," *Ram Accelerators*, Springer-Verlag, Heidelberg, Germany, 1998, pp. 97–104.
- <sup>4</sup>Giraud, M., Legendre, J. F., and Simon, G., "Ram Accelerator Studies in 90 mm Caliber," ISL Rept. CO 233/92, ISL, French-German Research Inst. of Saint Louis, Saint Louis, France, 1992.
- <sup>5</sup>Giraud, M., Legendre, J. F., and Henner, M., "RAMAC in Subdetonative Propulsion Mode: State of the ISL Studies," *Ram Accelerators*, Springer-Verlag, Heidelberg, Germany, 1998, pp. 65–77.
- <sup>6</sup>Elvander, J. E., Knowlen, C., and Bruckner, A. P., "High Acceleration Experiments Using a Multi-stage Ram Accelerator," *Ram Accelerators*, Springer-Verlag, Heidelberg, Germany, 1998, pp. 55–64.
- <sup>7</sup>Seiler, F., Patz, G., Smeets, G., and Srujijes, J., "Presentation of the Rail Tube Version II of ISL's RAMAC30," *Ram Accelerators*, Springer-Verlag, Heidelberg, Germany, 1998, pp. 79–87.
- <sup>8</sup>Sasoh, A., Hamate, Y., and Takayama, K., "Small-Bore Ram Accelerator Operation," *Journal of Propulsion and Power*, Vol. 17, No. 3, 2001, pp. 622–628.
- <sup>9</sup>Chang, X., Matsuoka, S., Watanabe, T., and Taki, S., "Ignition Study for Low Pressure Combustible Mixture in a Ram Accelerator," *Ram Accelerators*, Springer-Verlag, Heidelberg, Germany, 1998, pp. 105–109.
- <sup>10</sup>Liu Sen, Bai, Z. Y., Jian, H. X., Ping, X. H., and Bu, S. Q., "37-mm Bore Ram Accelerator of CARDC," *Ram Accelerators*, Springer-Verlag, Heidelberg, Germany, 1998, pp. 119–122.
- <sup>11</sup>Bruckner, A. P., Knowlen, C., Hertzberg, A., and Bogdanoff, D. W., "Operational Characteristics of the Thermally Choked Ram Accelerator," *Journal of Propulsion and Power*, Vol. 7, No. 5, 1991, pp. 828–836.
- <sup>12</sup>Legendre, J.-F., Giraud, M., and Henner, M., "Velocity Performance in RAMAC 90 Multistage Experiments," AIAA Paper, 98-3447, 1998.
- <sup>13</sup>Kruczynski, D. L., and Liberatore, F., "Experimental Investigation of High Pressure/Performance Ram Accelerator Operation," AIAA Paper, 96-2676, 1996.
- <sup>14</sup>Bruckner, A. P., "The Ram Accelerator: Overview and State of the Art," *Ram Accelerators*, Springer-Verlag, Heidelberg, Germany, 1998, pp. 1–23.
- <sup>15</sup>Bundy, C., Knowlen, C., and Bruckner, A. P., "Ram Accelerator Operating Characteristics at Elevated Fill Pressures," *Journal de Physique IV*, Vol. 10, Pr11, 2000, pp. 11–21.
- <sup>16</sup>Bundy, C., Knowlen, C., and Bruckner, A. P., "Ram Accelerator Operation at 15 to 20 MPa Fill Pressure," *Proceedings of the 18th International Colloquium on the Dynamics of Explosions and Reactive Systems* [CD-ROM], Univ. of Washington, 2001.
- <sup>17</sup>Knowlen, C., and Bruckner, A. P., "A Hugoniot Analysis of the Ram Accelerator," *Shock Waves, Proceedings of the 18th International Symposium on Shock Waves*, Springer-Verlag, Berlin-Heidelberg, 1992, pp. 617–622.
- <sup>18</sup>Knowlen, C., and Sasoh, A., "Ram Accelerator Performance Modeling," *Ram Accelerators*, Springer-Verlag, Heidelberg, Germany, 1998, pp. 25–37.
- <sup>19</sup>Sasoh, A., Higgins, A. J., Knowlen, C., and Bruckner, A. P., "Hollow Projectile Operation in the Ram Accelerator," *Journal of Propulsion and Power*, Vol. 12, No. 6, 1996, pp. 1183–1186.
- <sup>20</sup>Chang, X., Higgins, A., Schultz, E., and Bruckner, A., "Operation of Quasi-Two-Dimensional Projectiles in a Ram Accelerator," *Journal of Propulsion and Power*, Vol. 13, No. 6, 1997, pp. 802–804.
- <sup>21</sup>Yatsufusa, T., Fukahori, S., Yanase, T., Chang, X., and Taki, S., "Unstart Problem of Ram Accelerator in Thermally Choking Mode," *Journal of the Japan Society of Aeronautical and Space Sciences*, Vol. 49, No. 573, 2001, pp. 354–359 (in Japanese).
- <sup>22</sup>Hamate, Y., Sasoh, A., and Takayama, K., "Ram Accelerator Operations at Acceleration Level up to  $6 \times 10^4$  g," *Journal de Physique IV*, Vol. 10, Pr11, 2000, pp. 3–9.
- <sup>23</sup>Sasoh, A., Hirakata, S., Maemura, J., Hamate, Y., and Takayama, K., "Thermally Choked Operation in a 25-mm-Bore Ram Accelerator," *Ram Accelerators*, Springer-Verlag, Heidelberg, Germany, 1998, pp. 111–118.
- <sup>24</sup>Higgins, A. J., Knowlen, C., and Bruckner, A. P., "Ram Accelerator Operation Limits, Part 1: Identification of Limits," *Journal of Propulsion and Power*, Vol. 14, No. 6, 1998, pp. 951–958.
- <sup>25</sup>Schultz, E., Knowlen, C., and Bruckner, A. P., "Overview of the Subdetonative Ram Accelerator Starting Process," *Ram Accelerators*, Springer-Verlag, Heidelberg, Germany, 1998, pp. 189–203.
- <sup>26</sup>Schultz, E., Knowlen, C., and Bruckner, A. P., "Starting Envelope of the Subdetonative Ram Accelerator," *Journal of Propulsion and Power*, Vol. 16, No. 6, 2000, pp. 1040–1052.
- <sup>27</sup>Taylor, G. I., and Maccoll, J. W., "The Air Pressure on a Cone Moving at High Speeds," *Proceeding of the Royal Society of London, Series A: Mathematical and Physical Sciences*, Vol. 139, 1933, pp. 278–297.